Cerebrovascular Reactivity Mapping using Resting-State Functional MRI in Patient with gliomas.

Mei-Yu Yeh[1,2], Evan D H Gates[1], Ping Hou[1], Vinodh A. Kumar[3], Jason M. Johnson[3], Kyle R. Noll[4], Sujit S Prabhu[5], Sherise D. Ferguson[5], Ganesh Rao[5], Donald F. Schomer[3], Ho-Ling Liu[1]

[1]Department of Imaging Physics, The University of Texas MD Anderson Cancer Center, Houston, TX;
[2]Department of Biomedical Engineering and Environmental Sciences, National Tsing Hua University, Hsinchu Taiwan;
[3]Departments of Diagnostic Radiology, [4]Department of Neuro-oncology, [5]Department of Neurosurgery, The University of Texas MD Anderson Cancer Center, Houston, TX

INTRODUCTION

Lesion-induced neurovascular uncoupling (NVU) can lead to false negative results in clinical functional MRI (fMRI)[4]. Cerebrovascular reactivity (CVR) measured by using breath-hold (BH) MRI is a key indicator of the potential NUV, and therefore such procedure if recommended to accompany presurgical fMRI studies. However, BH MRI is often limited by patient performance [1]. Resting-state (rs) fMRI is an emerging technique for mapping eloquent functional areas for patients having compromised task performance in presurgical fMRI. This work proposes to use rs-fMRI for mapping the CVR in additional to the functional brain networks.

AIM

This study aimed to investigate the frequency range selection of resting-state (rs) fMRI signal fluctuations for the cerebrovascular reactivity (CVR) mapping in gliomas patients, and to compare the results with the CVR mapping with breath-hold (BH) MRI.

METHOD

Twenty-four patients with gliomas underwent the MRI study on a clinical 3T scanner. MRI scans included pre- and post-contrast T1-weighted imaging, fluid attenuated inversion recovery imaging, rs-fMRI (single-shot EPI, 180 dynamics, scan time = 6 mins) and BH MRI (single-shot EPI, 70 dynamics, 3 cycles of 15-s BH and 45-s rest). The rs-fMRI data were used to estimate CVR maps by using rs fluctuation of amplitude (RSFA, > 0.009 Hz) and amplitude of low frequency fluctuation (ALFF, 0.01-0.08 Hz)[4]. In addition, an RSFA map was generated after an automatic denoise process (RSFA_fix). The denoise procedure was conducted by using Independent component analysis and automatic classification in FIX (v1.06.12, Oxford, UK)[2]. CVR mapping with BH-MRI was performed by general linear model based on a respiratory response function. Tumor ROIs were determined by segmentation using a deep learning model and then in inspected/adjusted by a neuroradiologist. Dice index was calculated to evaluate the similarity between each of the rs-fMRI CVR maps and the CVR map obtained with the BH-MRI.

RESULTS

FIX independent component classification performance was shown in Figure 1. In the optimal threshold, when using the FIX standard model, the true positive rate (TPR) and the true negative rate(TNR) of 43.93% and 79.13%, respectively; and when using the patient training, the TPR and TNR of 82.51% and 81.17%, respectively. It is necessity to use the appropriate training of FIX in patient with gliomas. The Dice similarity between the RSFA without and with denoise inside normal tissue and lesion ROIs. We observed the ALFF maps with significant higher dice than RSFA maps in grey matter ROI (Dice=0.74,0.77) and white matter + Cerebrospinal fluid ROI (Dice=0.62, 0.64). On the other hand, we found the opposite results in the three difference characteristics lesions, in particular, there is a significant difference was found in edema ROI (Figure2). Figure 3 shows better spatial correspondence between the ALFF and CVR in normal regions. And discrepancies between the two were observed in the lesion. In contrast, the better agreement of RSFA and CVR in lesion ROI.

RESULTS

Table 1: Demography and histology, tumor grade and tumor location for the patients were evaluated in this study.

Patient No.	Gender	Age	Histopathology	WHO tumor grade	Tumor Location
1	M	44	anaplastic astrocytoma	III	right frontal
2	F	31	ganglioglioma	I	left superior temporal
3	M	44	diffuse glioma	II	left temporal
4	F	45	glioblastoma	IV	left posterior frontal
5	F	32	astrocytoma	II	left frontal temporal
6	F	58	astrocytoma	III	left temporal parietal
7	M	24	astrocytoma	II	left frontal temporal
8	M	58	glioblastoma	IV	left frontal temporal
9	F	27	astrocytoma	II	left parietal
10	F	34	oligodendroglioma	II	left frontal
11	M	66	glioblastoma	IV	right frontal
12	F	41	glioblastoma	IV	left temporal
13	F	53	anaplastic astrocytoma	III	left insular
14	F	35	astrocytoma	II	left frontal
15	M	34	oligodendroglioma	II	left frontal temporal
16	M	66	glioblastoma	IV	left posterior frontal
17	M	57	astrocytoma	III	left temporal
18	F	43	oligodendroglioma	II	left parietal
19	F	65	glioblastoma	IV	left temporal
20	M	61	astrocytoma	IV	left temporal
21	M	61	glioblastoma	IV	left temporal
22	M	57	astrocytoma	II	left temporal
23	M	33	astrocytoma	II	left temporal
24	F	42	oligodendroglioma	II	left frontal temporal

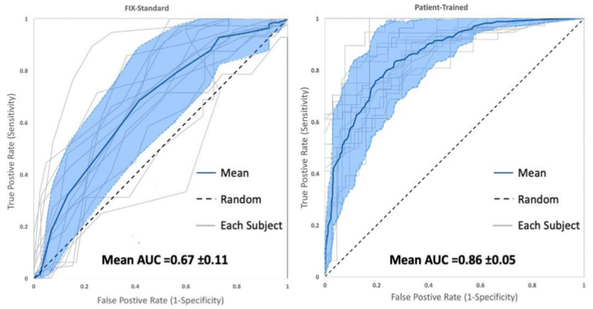

Figure 1 FIX independent component classification performance in ROC curve on the patients with Gliomas of rs-fMRI data, after (A) FIX-Standard and (B) Patient training.

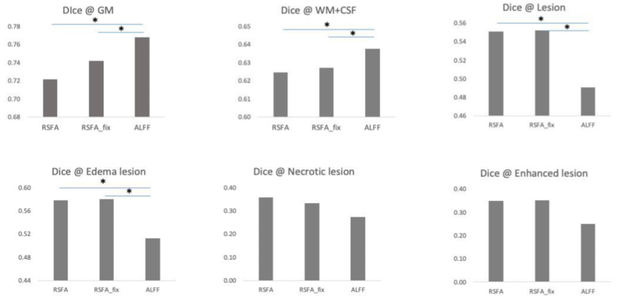

Figure 2
The agreement (Dice) between CVR map and two RSFA maps (with and without removing noise by FIX) in different ROIs.

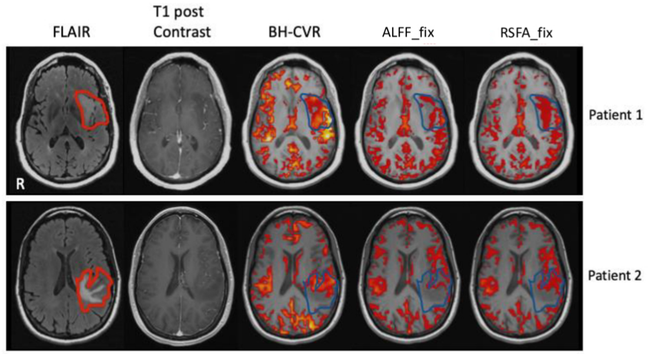

Figure 3
The first column shows the lesion on the FLAIR structural images. The second, third and last columns show cerebrovascular reactivity (CVR), ALFF and RSFA with denoise maps on T1-weighted image .

CONCLUSIONS

The ALFF performed well for CVR mapping in normal tissues, whereas a wider frequency range needed to be incorporated in diseased tissues. The overall lower dice in lesions than in normal tissues requires further studies.

The ALFF maps might be a good mapping for CVR maps in normal tissue. The range of frequency will affect the agreement of RSFA and CVR maps. It is need to be considered the contribution from higher frequency in the lesion.

ACKNOWLEDGEMENTS

Thank you to the MD Anderson team.

REFERENCES

[1] Sridhar S.KannurpattiBharat B.Biswal. Detection and scaling of task-induced fMRI-BOLD response using resting state fluctuations. NeuroImage.2008;40:1567-1574
G. Salimi-Khorshidi, G. Douaud, C.F. Beckmann, M.F. Glasser, L. Griffanti S.M. Smith. Automatic denoising of functional MRI data: Combining independent component analysis and hierarchical fusion of classifiers. NeuroImage.2014; 90:449-68, 2014
[2] L. Griffanti, G. Salimi-Khorshidi, C.F. Beckmann, E.J. Auerbach, G. Douaud, C.E. Sexton, E. Zsoldos, K. Ebmeier, N. Filippini, C.E. Mackay, S. Moeller, J.G. Xu, E. Yacoub, G. Baselli, K. Ugurbil, K.L. Miller, and S.M. Smith. ICA-based artefact removal and accelerated fMRI acquisition for improved resting state network imaging. NeuroImage. 2014; 95:232-47
[3] Zang YF, He Y, Zhu CZ, Cao QJ, Sui MQ, Liang M, Tian LX, Jiang TZ, Wang YF. Altered baseline brain activity in children with ADHD revealed by resting-state functional MRI. Brain Dev. 2007; 29(2):83-91
[4] Craig M. Bennett and Michael B. Miller. How reliable are the results from functional magnetic resonance imaging? Ann. N.Y. Acad. Sci. ISSN 0077-8923

CONTACT INFORMATION

myeh@mdanderson.org or maiyu730521@gmail.com